
Label Alignment Regularization for Distribution Shift

Ehsan Imani
Huawei
Noah’s Ark Lab

Guojun Zhang
Huawei
Noah’s Ark Lab

Jun Luo
Huawei
Noah’s Ark Lab

Pascal Poupart
University of Waterloo

Yangchen Pan
Huawei
Noah’s Ark Lab

Abstract

Recent work reported the label alignment property in a supervised learning setting: the vector of all labels in the dataset is mostly in the span of the top few singular vectors of the data matrix. Inspired by this observation, we derive a regularization method for unsupervised domain adaptation. Instead of regularizing representation learning as done by popular domain adaptation methods, we regularize the classifier so that the target domain predictions can to some extent “align” with the top singular vectors of the unsupervised data matrix from the target domain. In a linear regression setting, we theoretically justify the label alignment property and characterize the optimality of the solution of our regularization by bounding its distance to the optimal solution. We conduct experiments to show that our method can work well on the label shift problems, where classic domain adaptation methods are known to fail. We also report mild improvement over domain adaptation baselines on a set of commonly seen MNIST-USPS domain adaptation tasks and on cross-lingual sentiment analysis tasks.

1 Introduction

Unsupervised domain adaptation studies knowledge transfer from a source domain with labeled data, to a target domain with unlabeled data, where the model will be deployed and evaluated (Ben-David et al., 2010; Mansour et al., 2009). This difference between the two domains, called domain shift, arises in many applications of machine learning. A document classification or sentiment analysis model for an under-resourced language can benefit from a large corpus for a different language. A personal healthcare

system is often trained on a group of users different from its target users. A real-world robot’s predictions or decision-making can improve through safe and less costly interactions with a simulator (Pires et al., 2019; Ganin et al., 2016; Peng et al., 2018).

Prevalence of domain shift in machine learning has inspired a large body of algorithmic and theoretical research on domain adaptation. Ganin et al. (2016) and Zhang et al. (2019) formulated the difference between the source and the target domain with the notion of \mathcal{H} -divergence and Margin Disparity Discrepancy and provided generalization bounds that relate performance on the two domains. Acuna et al. (2021) extended these results to a more general notion of f -divergence. Adversarial domain adaptation algorithms are motivated by these theoretical findings and aim to learn representations that achieve high performance in the source domain while being invariant to the shift between the source and the target domain (Zhang et al., 2017b; Conneau et al., 2018; Long et al., 2015; Pei et al., 2018).

The aforementioned feature-matching approach assumes that the optimal joint risk between the source and target is small. This assumption fails when the conditional distribution of the labels given input is different between source and target domains—which we call *label shift*. An example is when in the source domain labels are much more imbalanced than in the target domain. For instance, Zhao et al. (2019) identified that under such label distribution shift, the optimal joint risk can be quite large and they empirically show the failure of domain adaptation methods on MNIST-USPS digit datasets. Johansson et al. (2019) also pointed out the limitation of matching feature representations by pointing out its inconsistency, and thus tendency for high target errors.

In this work, we take a different approach to domain adaptation that relies on label alignment, the property that the labels align with the top singular vectors of the representation. Rather than learning an invariant representation, our proposed algorithm adjusts the classifier to the target domain by removing the effect of label alignment in the source domain on the classifier and enforcing this property on the target domain predictions.

We describe label alignment phenomenon in Section 2, and outline the proposed method in Section 3. Section 4 provides a bound on the difference between the solution found by our regularization and the true solution in a linear regression setting. Section 5 reviews related work. In Section 6, we first provide a synthetic example where the proposed regularizer shows a clear advantage. We then experiment with imbalanced MNIST-USPS binary classification tasks and find that our method, unlike the domain-adversarial baseline, is robust to label shift. Finally, we evaluate our algorithm on cross-lingual sentiment analysis tasks and observe improved F_1 score over training without using our regularization and using an adversarial domain adaptation baseline.

2 Background: Label Alignment

In this section, we briefly review the standard linear regression problem and define relevant notation to explain the label alignment property (Imani et al., 2022).

2.1 Linear Regression and Notations

We consider a dataset with n samples, (possibly learned and nonlinear) representation matrix $\Phi \in \mathbb{R}^{n \times d}$ and label vector $y \in \mathbb{R}^n$ from a source domain. Denote the model’s weights as $w \in \mathbb{R}^d$, we study the linear regression problem:

$$\min_w \|\Phi w - y\|^2 \quad (1)$$

Without loss of generality, we replace the bias unit with a constant feature in the representation matrix to avoid studying the unit separately. The model will be evaluated on a test set sampled from the target domain.

The singular value decomposition (SVD) of a representation matrix Φ is

$$\Phi = U \Sigma V^\top = \sum_{i=1}^d \sigma_i u_i v_i^\top, \text{ where}$$

$$\Sigma = \begin{bmatrix} \sigma_1 & & & \\ & \ddots & & \\ & & \sigma_d & \\ & & & \mathbf{0}_{n-d,d} \end{bmatrix} \in \mathbb{R}^{n \times d}$$

is a rectangular diagonal matrix whose main diagonal consists of singular values $\sigma_1, \dots, \sigma_d$ in descending order and

$$U = [u_1, \dots, u_n] \in \mathbb{R}^{n \times n} \text{ and } V = [v_1, \dots, v_d] \in \mathbb{R}^{d \times d}$$

are orthogonal matrices whose columns $u_i \in \mathbb{R}^n$ and $v_j \in \mathbb{R}^d$ are the corresponding left and right singular vectors. In principal component analysis (Pearson, 1901), v_1, \dots, v_k

are also known as the first k principal components. For a vector a and orthonormal basis B , a^B is a shorthand for $B^\top a$, the representation of a with row vectors of B . We use $r(\cdot)$ to denote the rank of a matrix.

2.2 Label Alignment

Label alignment is specified in terms of the singular vectors of Φ and label vector y . The left singular vectors of Φ , $\{u_1, \dots, u_n\}$ form an orthonormal basis that spans the n -dimensional space. The label vector $y \in \mathbb{R}^n$ can be decomposed in this basis with:

$$y = U y^U = y_1^U u_1 + \dots + y_n^U u_n. \quad (2)$$

Here y_i^U is the i^{th} component of vector $y^U \in \mathbb{R}^n$ for $i \in \{1 \dots n\}$.

Label alignment (Imani et al., 2022) is a relationship between the labels and the representation where the variation in the labels are mostly along the top principal components of the representation. For our purpose we give the following definition and verify that it approximately holds in a number of real-world tasks. A dataset has *label alignment* with rank k if for $k \ll r(\Phi)$ we have $y_i^U u_i = 0, \forall i \in \{k+1, \dots, d\}$.

In Table 1 we investigate this property in binary classification tasks (with ± 1 labels) and regression tasks. In this table $k(\epsilon)$ means the smallest k where $\sqrt{\sum_{i=k+1}^d (y_i^U)^2} < \epsilon \sqrt{\sum_{i=1}^d (y_i^U)^2}$. If $k(\epsilon)$ is small for a small ϵ then the projection of the label vector on the span of Φ is mostly in the span of the first few singular vectors. In all the ten tasks less than half the singular vectors with nonzero singular values already span more than 90 percent of the norm of the projection of y on the span of Φ . The number $k(0.1)$ is remarkably small, less than 10, in seven out of the ten tasks. In Appendix A we show emergence of this property in a controlled setting where a large number of features are correlated with the labels.

It should be noted that similar label alignment phenomenon has been also observed in a deep learning setting. Recent work in the Neural Tangent Kernel (NTK) literature has observed that in common datasets the label vector is largely within the span of the top eigenvectors of the NTK Gram matrix (Arora et al., 2019). In contrast, a randomized label vector would be more or less uniformly aligned with all eigenvectors. Fast optimization and better generalization of neural networks on true labels compared to random labels is attributed to this alignment between the labels and the top eigenvectors of the NTK (Canatar et al., 2021; Arora et al., 2019; Jacot et al., 2018; Rahaman et al., 2019; Oymak et al., 2019; Zhang et al., 2017a). More recently, Baratin et al. (2021) and Ortiz-Jiménez et al. (2021) noted that training a finite-width neural network makes the alignment between the network’s kernel and the task even

Task	n	d	$r(\Phi)$	$k(0.1)$
UCI CT Scan	10000	385	372	12
Song Year	10000	91	91	6
Bike Sharing	10000	13	13	4
MNIST	12665	785	580	2
USPS	2199	257	257	2
Task	n	d	$r(\Phi)$	$k(0.1)$
CIFAR-10	10000	513	513	7
CIFAR-100	1000	513	513	7
STL-10	1000	513	513	2
XED (English)	6525	769	769	231
AG News	10000	769	769	40

Table 1: Label alignment in real-world tasks. The table at the top uses the original features in the dataset and the table at the bottom uses features extracted from neural networks. UCI CT Scan, Song Year, and Bike Sharing are regression tasks and the rest are binary classification. We used the first two classes of multi-class classification datasets to create a binary classification task. Other details about the datasets are in Appendix B. In all of these tasks, a large portion of the label vector is in the span of a relatively small set of top singular vectors (compared to the rank).

stronger. Imani et al. (2022) observed a similar behavior in neural network hidden representations, indicating that training the neural network aligns the top singular vectors of the hidden representations to the task.

2.3 Reformulating the Regression Objective

We now describe how to reformulate the linear regression objective function by using the label alignment property. This reformulation shows that the linear regression objective is implicitly enforcing the label alignment property on the source domain (i.e., the training data) and this encourages us to further derive our domain adaptation regularization on the target domain.

Our linear regression objective (1) can be rewritten by the following steps.

$$\begin{aligned}
 \min_w \|\Phi w - y\|^2 &= \min_w \|U\Sigma V^\top w - y\|^2 \\
 &= \min_w \|\Sigma V^\top w - U^\top y\|^2 \\
 &= \min_w \|\Sigma w^V - y^U\|^2 \\
 &= \min_w \sum_{i=1}^d (\sigma_i w_i^V - y_i^U)^2 + \sum_{i=d+1}^n (y_i^U)^2.
 \end{aligned} \tag{3}$$

In the second line, since U is an orthogonal matrix, we have $UU^\top = \mathbb{I}$ and $\|Ux\| = \|x\|$ for any vector x . The last equality holds because the matrix Σ has zero rows after the first d rows.

Assume the label alignment property holds for the first $k < d$ singular vectors. Then $y_i^U = 0, \forall i \in k+1, \dots, d$. Hence the first term in objective (3) can be further decomposed to

$$\sum_{i=1}^d (\sigma_i w_i^V - y_i^U)^2 \tag{4}$$

$$= \sum_{i=1}^k (\sigma_i w_i^V - y_i^U)^2 + \sum_{i=k+1}^d \sigma_i^2 (w_i^V)^2. \tag{5}$$

Plugging this decomposition into the above objective (3) and drop the last term, we get

$$\min_w \sum_{i=1}^k (\sigma_i w_i^V - y_i^U)^2 + \sum_{i=k+1}^d \sigma_i^2 (w_i^V)^2. \tag{6}$$

Note that the last term $\sum_{i=k+1}^d (y_i^U)^2$ can be dropped as it is a constant and does not affect the optimization. We can interpret the first term in the rewritten objective (6) as linear regression on a smaller subspace and the second term as a regularization term implicitly enforcing label alignment property on the training data (Φ, y) .

The latter is because minimizing the second term has the effect of regularizing the predictions so they likely align with the top singular vectors. This is because: $y = \Phi w = U\Sigma V^\top w$ and therefore $U^\top y = \Sigma V^\top w$ and this can be written as $y^U = \Sigma w^V$ by using the shorthand notations. For the i th component in vector y^U , we have $u_i^\top y = \sigma_i v_i^\top w$. Minimizing w_i^V for $i \in \{k+1, \dots, d\}$ will reduce the corresponding y_i^U and leave y_i^U for those components $i < k+1$. We call the second term $\sum_{i=k+1}^d \sigma_i^2 (w_i^V)^2$ *label alignment regularization*.

The derivation above shows that when minimizing the original mean squared error for linear regression, we implicitly use label alignment regularization on the training data (source domain data). In the next section, we introduce this regularization into the target domain.

3 Label Alignment for Domain Adaptation

This section describes our approach for domain adaptation by enforcing the label alignment property.

In unsupervised domain adaptation, we have a labeled dataset (Φ, y) and an unlabeled dataset $\tilde{\Phi}$ with the corresponding label vector \tilde{y} unknown. From (6), we know that enforcing the label alignment property does not require knowing the labels \tilde{y} . This inspires our key idea of improving the generalization on the target domain: we can use the unlabeled part to enforce the label alignment property.

Assuming $(\tilde{\Phi}, \tilde{y})$ satisfies the label alignment property with rank \tilde{k} , we can put together the supervised part of the source domain and unsupervised part of the target domain

to form the objective:

$$\min_w \|\Phi w - y\|^2 + \sum_{i=\tilde{k}+1}^d \tilde{\sigma}_i^2(w_i^{\tilde{V}})^2. \quad (7)$$

The second term $\sum_{i=\tilde{k}+1}^d \tilde{\sigma}_i^2(w_i^{\tilde{V}})^2$ is the *label alignment regularization on the target domain*.

As we explained in the previous section, the first term (i.e. the standard regression part) in the above objective implicitly enforces the label alignment property (with rank k) on the source domain. If we expand (7) by using the reformulated linear regression objective (6), we have:

$$\min_w \sum_{i=1}^k (\sigma_i w_i^V - y_i^U)^2 + \sum_{i=k+1}^d \sigma_i^2(w_i^V)^2 + \sum_{i=\tilde{k}+1}^d \tilde{\sigma}_i^2(w_i^{\tilde{V}})^2. \quad (8)$$

Therefore, we have actually done the regularization *twice*: one with the source domain and one with the target domain. We explicitly remove the label alignment regularization on the source domain and arrive at the final objective function:

$$\min_w \|\Phi w - y\|^2 - \sum_{i=k+1}^d \sigma_i^2(w_i^V)^2 + \lambda \sum_{i=\tilde{k}+1}^d \tilde{\sigma}_i^2(w_i^{\tilde{V}})^2. \quad (9)$$

Algorithm 1 shows the pseudo-code. The objective to be minimized has three terms and the parameter λ controls the relative importance of the regularizer. The first term is the loss that uses the labeled data from the source domain. Following the recent evidence on viability of the squared error loss for classification (Hui & Belkin, 2020), we use the squared error in both regression tasks and binary classification tasks. We use ± 1 labels in binary classification as these labels showed the label alignment property in Table 1. The second term removes implicit regularization from the source domain. The third term is the proposed regularizer that uses the unlabeled data from the target domain. Given a hyperparameter \tilde{k} , this term minimizes the projection of the weights on singular vectors $\tilde{v}_{k:d}$ to enforce the desired property on the model's predictions for the target domain.

4 Theoretical Insight: Optimality Bound

This section theoretically characterizes the optimality of our algorithm's solution.

Setting the regularization weight to one, the optimization problem for (9) can be rewritten in a matrix form:

$$\min_w \|\Phi w - y\|^2 - w^\top (S - S_k) w + w^\top (\tilde{S} - \tilde{S}_{\tilde{k}}) w, \quad (10)$$

Algorithm 1 Domain Adaptation with Label Alignment Regularization

Get data Φ , y , $\tilde{\Phi}$, and hyperparameters t , α , k , \tilde{k} , λ

Compute covariance matrices $\Phi^\top \Phi$ and $\tilde{\Phi}^\top \tilde{\Phi}$

Perform eigendecomposition of $\Phi^\top \Phi$ and $\tilde{\Phi}^\top \tilde{\Phi}$ to get the $\sigma_{k+1:d}$, $\tilde{\sigma}_{\tilde{k}+1:d}$, $\tilde{v}_{k+1:d}$ and $\tilde{v}_{\tilde{k}+1:d}$

Initialize w to zero

for t iterations **do**

 Perform gradient step with respect to $\|\Phi w - y\|^2 - \sum_{i=k+1}^d \sigma_i^2(w_i^V)^2 + \lambda \sum_{i=\tilde{k}+1}^d \tilde{\sigma}_i^2(w_i^{\tilde{V}})^2$ with step-size α and update w

end for

where $\tilde{S} = \tilde{\Phi}^\top \tilde{\Phi}$ is the Gram matrix of $\tilde{\Phi}$, $\tilde{S}_{\tilde{k}} = \tilde{\Phi}_{\tilde{k}}^\top \tilde{\Phi}_{\tilde{k}}$ is the Gram matrix of $\tilde{\Phi}_{\tilde{k}}$. Here $\tilde{\Phi}_{\tilde{k}}$ is the truncated SVD of $\tilde{\Phi}$, which is the closed approximation of $\tilde{\Phi}$ with rank \tilde{k} . $\tilde{S} - \tilde{S}_{\tilde{k}}$ is thus the residual part after truncation. The optimal solution for the problem above is:

$$\widehat{w}^* = (S_k + \tilde{S} - \tilde{S}_{\tilde{k}})^{-1} \Phi^\top y, \quad (11)$$

where $S = \Phi^\top \Phi$. Suppose we have the optimal solution, we ask the following question: how good does it perform on the unlabeled dataset $\tilde{\Phi}$? To achieve this goal we need to provide an upper bound of $\|\tilde{\Phi} \widehat{w}^* - \tilde{y}\|^2$, which can be given using the domain shift and the label alignment property.

Let us now provide a generalization bound for linear regression. We prove that the optimal test regression estimator is not far away from the optimum in (9), under certain assumptions:

Theorem 1 *Suppose the optimal solution of $\|\tilde{\Phi} w - \tilde{y}\|^2$ is $w_{\mathcal{T}}^*$ and the learned classifier has norm $\|\widehat{w}^*\| \leq B$. If the Gram matrix $\tilde{S} = \tilde{\Phi}^\top \tilde{\Phi}$ is non-singular and σ_{\min} is the minimal singular value, then the distance between the optimal target solution w^* and the learned solution \widehat{w}^* is bounded:*

$$\|\widehat{w}^* - w_{\mathcal{T}}^*\| \leq \frac{1}{\sigma_{\min}} \cdot (\|\Phi^\top y - \tilde{\Phi}^\top \tilde{y}\| + B \|S_k - \tilde{S}_{\tilde{k}}\|). \quad (12)$$

Proof We can obtain the solution for the target problem:

$$w_{\mathcal{T}}^* = \tilde{S}^{-1} \tilde{\Phi}^\top \tilde{y}. \quad (13)$$

The two equations (11) and (13) can be rewritten as:

$$(S_k + \tilde{S} - \tilde{S}_{\tilde{k}}) \widehat{w}^* = \Phi^\top y, \quad (14)$$

$$\tilde{S} w_{\mathcal{T}}^* = \tilde{\Phi}^\top \tilde{y}. \quad (15)$$

Subtracting the second equation from the first, we have:

$$\tilde{S} (\widehat{w}^* - w_{\mathcal{T}}^*) = (\Phi^\top y - \tilde{\Phi}^\top \tilde{y}) - (S_k - \tilde{S}_{\tilde{k}}) \widehat{w}^* \quad (16)$$

$$\widehat{w}^* - w_{\mathcal{T}}^* = \tilde{S}^{-1} ((\Phi^\top y - \tilde{\Phi}^\top \tilde{y}) - (S_k - \tilde{S}_{\tilde{k}}) \widehat{w}^*). \quad (17)$$

Taking the norm on both sides and applying the triangle inequality we obtain the claimed result. ■

We can obtain a similar theorem to bound the difference between the target solution and the *unregularized* source solution.

Theorem 2 *Suppose the optimal solution of the unregularized $\|\Phi w - y\|^2$ is w_S^* , with its norm $\leq B_S$. With the same settings as Theorem 1, the distance between the optimal target solution w^* and the learned solution \widehat{w}^* is bounded:*

$$\|w_S^* - w_T^*\| \leq \sigma_{\min}^{-1} \cdot (\|\Phi^\top y - \tilde{\Phi}^\top \tilde{y}\| + B_S \|S - \tilde{S}\|). \quad (18)$$

Proof The proof is similar to the proof of Theorem 1 and we omit here. ■

Suppose $\|\Phi^\top y - \tilde{\Phi}^\top \tilde{y}\|$ is small. Comparing Theorem 1 (with $\lambda = 1$) and Theorem 2 we find that:

- If the *truncated* Gram matrices are similar, our regularization scheme can learn a classifier that is close to the true optimal classifier;
- If the *original* Gram matrices are similar, the unregularized scheme can learn a classifier that is close to the true optimal classifier.

Moreover, by gradually increasing k and \tilde{k} to the feature dimension d , we can obtain an interpolation between our regularization scheme and the unregularized scheme.

5 Related Work

The dominant approach to domain adaptation is learning domain-invariant representations that are “similar” in some sense between source and target domains (Tzeng et al., 2014; Zhuang et al., 2015; Ghifary et al., 2016; Long et al., 2016, 2017; Benaim & Wolf, 2017; Bousmalis et al., 2017; Courty et al., 2017; Motiian et al., 2017; Rebuffi et al., 2017; Saito et al., 2017; Zhang et al., 2019). Different methods differ in how the invariance property is enforced, which typically includes how the similarity is defined and implemented.

The result by Ben-David et al. (2010) provides a general theoretical guidance regarding how to learn the domain-invariant representations. The basic idea is to make the joint error of the best hypothesis on the two domains on the invariant representation small. Low joint error in the domain-adversarial model is crucial to the model’s performance on the target domain.

The popular domain-adversarial methods achieve domain-invariant representations based on the idea of adversarial

models (Long et al., 2015; Zhuang et al., 2017; Lee et al., 2019; Damodaran et al., 2018; Acuna et al., 2021). Specifically, Long et al. (2015) adversarially learn representations to distinguish the data points from the source and target domain while minimizing the supervised loss on the source domain. Conneau et al. (2018) use a domain-adversarial approach to align representations of the source and target domains in a shared space. They transform the source embeddings with a linear mapping that is encouraged to be orthogonal. The domain-adversarial model then generates pseudo-labels on the target domain for additional refinement steps.

There are various similarity or distance measures to define a loss function for enforcing invariant representations. For example, Zhuang et al. (2017) and Meng et al. (2018) minimize the KL-divergence and Lee et al. (2019) and Damodaran et al. (2018) minimize the Wasserstein distance. Sun & Saenko (2016) minimize the ℓ_2 distance between the covariance matrices of the source and target domain representations. Long et al. (2015) minimize Maximum Mean Discrepancy between source and target domain hidden representations embedded with a kernel.

However, despite flourished literature in representation-based domain adaptation methods, they have critical limitations. Zhao et al. (2019) and Johansson et al. (2019) created synthetic examples where a domain-adversarial model that minimizes the source domain supervised loss with an invariant representation still fails on the target domain. Zhao et al. (2019) also observed similar failures in digit classification tasks where the source domain, unlike the target domain, is severely imbalanced.

Domain-adaptation methods that do not rely on representation learning are less studied and can be applied in highly restricted settings. For example, importance sampling (Shimodaira, 2000) assumes covariate shift, that is, the label conditional distributions are the same between the two domains while the input distributions can differ, and further requires mild domain-shift: the target domain is within the source domain’s support. This classical method reweights the source domain data points in the supervised objective to account for the shift in the input distributions.

There are diverse settings to study domain adaptation problems. In classification problems, closed set domain adaptation assumes the same categories between the two domains while open-set domain adaptation assumes that the two domains only share a subset of their categories (Panareda Busto & Gall, 2017). Unsupervised, semi-supervised, and supervised domain adaptation assume that the data from the target domain is fully unlabeled, partly labeled, and fully labeled respectively (Ganin et al., 2016). Two related problems to domain adaptation are multi-target domain adaptation where there are multiple target domains (Gholami et al., 2020) and domain generalization where

several source domains are sampled from a distribution over tasks and the goal is to generalize to a previously unseen domain from this distribution (Blanchard et al., 2011; Gulrajani & Lopez-Paz, 2021).

6 Experiments

In this section, we first design a synthetic dataset to verify that our regularizer is indeed beneficial in a distribution shift setting by adjusting the classifier. Then, we demonstrate the effectiveness of our method on a well-known benchmark where classic domain-adversarial methods are known to fail (Zhao et al., 2019). Last, we show our algorithm’s practical utility in a cross-lingual sentiment classification task.

6.1 Synthetic Data

We create a distribution shift scenario where the alignment property is present in the labeled data distribution (Figure 1). For the source domain (a), the input is sampled from a two dimensional Gaussian distribution. The distribution is more spread out in the direction of the first principal component (see the black arrows) which corresponds to a larger singular value. In this task the two classes are separated along this direction as shown in the figure. The resulting vector of all labels is mostly in the direction of the first left singular vector of the representation matrix. We rotate the input by 45 degrees to create the target distribution in (b).

We then run the proposed algorithm with hyperparameters $k = \tilde{k} = 1$ and different values of λ and compared it with the ℓ_2 regularizer and a domain-adversarial baseline DANN (Ganin et al., 2016) with one hidden layer of width 64. Figures 1 (b) to (d) show the results. Further details are in Appendix B. In Figure 1 (b) we see that the solution without regularization separates the classes as they are separated in the source domain. The proposed algorithm finds a separating hyperplane that matches how the classes are separated in the target domain. In (c), increasing the regularization weight in our method reduces the distance to the optimal weights on the target domain while the ℓ_2 regularizer cannot achieve this reduction. Finally, (d) shows that our regularizer surpasses both the ℓ_2 regularizer and the domain-adversarial baseline and achieves near perfect classification on the target domain in this example.

6.2 MNIST-USPS

The experiments in Table 2 consider binary classification tasks from the MNIST-USPS domain adaptation benchmark with linear and shallow models. Both MNIST and USPS are digit classification datasets with 10 classes and therefore 45 binary classification tasks between two digits. In MNIST, the input is a 28x28 grayscale image flattened to a 784 dimensional vector. USPS images are 16x16 and we

resize them to 28x28 and flatten each input to a 784 vector similarly.

Each column of the table is the average accuracy over 45 domain adaptation tasks. In the first column, the source domain (fully labeled) is a pair of digits from MNIST and the target domain (fully unlabeled) is the same pair, but from USPS. The datasets for the source and target domains are reversed in the second column. The last three columns are like the second column except that, in binary classification between two digits, only a certain ratio of the lower digit in the source domain, as indicated in the header, is used. This subsampling creates a large degree of label shift that, as Zhao et al. (2019) observed, poses a challenge to domain-adversarial methods.

We use the train split of the dataset for the source domain and the test split of the other dataset for the target domain. A small set of 100 labeled points from the target domain is used for hyperparameter selection as we have not developed a fully unsupervised hyperparameter selection strategy. However, we give the baseline the same validation set to keep the experiment fair.

The first two rows show the performance of the domain-adversarial method DANN (Ganin et al., 2016) with one hidden layer on these tasks. (Deeper neural networks performed worse on the highly imbalanced tasks in our preliminary experiments.) The first row is the average target domain accuracy of a two-layer ReLU neural network trained purely on the source domain. In the second row, the domain-adversarial objective is added to reduce domain shift in the hidden representation. DANN improves accuracy in both $U \rightarrow M$ and $M \rightarrow U$. In the cases with subsampling, however, DANN consistently hurts performance. The third and fourth row show the performance of a linear method with or without our regularizer. Using our regularizer improves performance in all columns and outperforms all the models in the other rows in the cases with high label shift.

We then investigate why DANN hurts performance in cases with severe label shift. Table 3 shows average source domain accuracy and domain classifier accuracy of DANN on these tasks. Average source accuracy remains above 95% and average domain classifier remains close to 50%, indicating that DANN has managed to learn a representation that is suitable for the source domain and maps the points from the source and target domain close to each other. The large drop in DANN’s performance can be attributed to the fact that the representation maps positive points in the source domain close to negative points in the target domain and vice-versa and therefore the joint error of the best hypothesis on the two domains (as described in Section 5) is large. We verify this by training a nearest neighbor (1-NN) classifier on the learned representation in the subsampled settings. The 1-NN classifier uses the source domain rep-

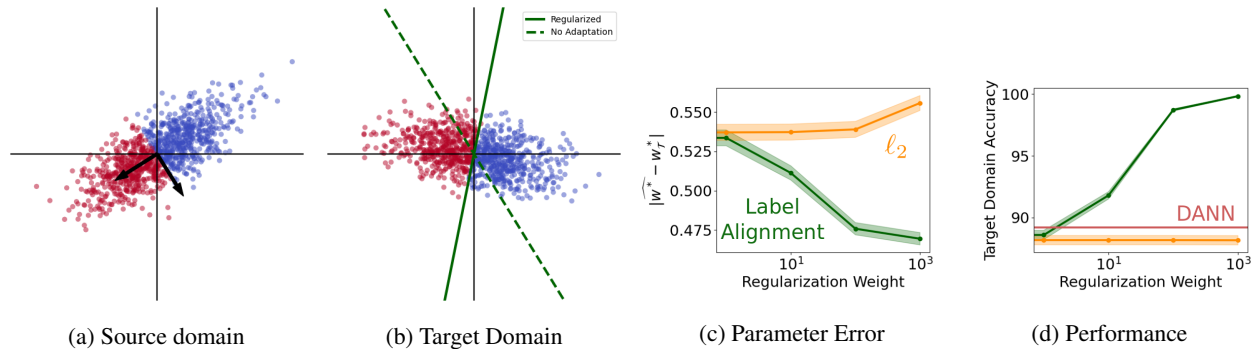


Figure 1: (a) Source domain. The black arrows show principal components. (b) Target domain. The green lines show separating hyperplanes found without using any regularization (dashed) and with our regularizer with $\lambda = 10^3$ (solid). (c) Distance between the estimated and the optimal weights. The proposed regularizer reduces this distance. (d) Performance on the target domain. The x axis is the regularization coefficient for ℓ_2 regularization and λ for the proposed regularizer. The red line shows the performance of DANN. The proposed regularizer achieves near perfect accuracy on this domain. Shaded areas are standard errors over 10 runs. Variations in target accuracy of DANN are near zero.

representations as the training data and the target domain representations as the test data. The accuracy of this classifier will suffer if in the learned representation the source domain points from one class are mapped close to the target domain points from the other class. The third row in the table, which is averaged over the 45 tasks like the other results, shows a noticeable drop in the performance of the 1-NN classifier and indicates that this problem is present in the learned embeddings under label shift.

6.3 Cross-Lingual Sentiment Classification

This section includes cross-lingual sentiment analysis experiments on deep features. XED (Öhman et al., 2020) is a sentence-level sentiment analysis dataset consisting of 32 languages. The sentences in the dataset are labeled with one or more emotions *anger*, *anticipation*, *disgust*, *fear*, *joy*, *sadness*, *surprise*, and *trust*. Following the author’s guidelines we turn these multi-label classification tasks to binary classification by labeling data points positive if their original labels only include *anticipation*, *joy*, and *trust*, and negative if the original labels only include *anger*, *disgust*, *fear*, and *sadness*. (*Surprise* is discarded.) We use English as the source domain and another language as the target domain and create 9 domain adaptation tasks. We perform 5 runs and in each one 100 points are randomly sampled from the target domain for validation and the rest are used for evaluation. The representations for the source and target domain are 768-dimensional sentence embeddings obtained with BERT (Devlin et al., 2019) models pre-trained on the corresponding languages.

Table 4 shows F_1 scores for the nine tasks and the average score over the tasks. In the first and second row a one-layer linear regression or logistic regression model is trained purely on the source domain using ± 1 labels. In

the third and fourth row, a one-layer linear regression or logistic regression model is trained in the same manner except that the source and target data points are mapped to the same space using the domain-adversarial method by Conneau et al. (2018) as described in Section 5. We picked this baseline since it is motivated for Natural Language Processing tasks and has shown promising results in this domain. In the last row we employ our regularizer on the linear regression model instead of employing the domain-adversarial method on the representations. The proposed regularizer achieves the highest F_1 score on seven out of the nine tasks as well as on average over the tasks.

7 Discussion

In this work, we proposed a domain adaptation regularization method based on the observation of label alignment property—the label vector of a dataset usually lies in the top singular vectors of the feature matrix. We show that a regression algorithm in a standard supervised learning task actually contains an implicit regularization method to enforce such a property. Then we demonstrate how we can adapt such a regularization method in a domain adaptation setting. A critical difference between our algorithm and the conventional domain adaptation method is that we do not use regularization to adjust the representation learning. And we observe that our algorithm does work well in the label shift setting, where the conventional representation-based domain adaptation method fails. We also report mild improvement over baselines on some common domain adaptation tasks.

Immediate next steps are providing an unsupervised hyperparameter selection strategy and extension to multi-class classification. Other future directions are to investigate the combination of our method and the conventional

Label Alignment Regularization for Distribution Shift

	U → M	M → U	0.3 → U	0.2 → U	0.1 → U
No Adaptation (NN)	77.85	84.88	83.36	72.84	53.58
DANN	83.93	86.69	78.05	64.2	47.27
No Adaptation (Linear)	78.68	83.84	80.99	79.47	75.41
Label Alignment Regularizer	81.97	88.96	86.99	84.84	82.71

Table 2: Accuracies on MNIST-USPS benchmark. Each column is averaged over the 45 binary classification tasks. M and U indicate MNIST and USPS. Ratios indicate MNIST tasks where one digit is subsampled. In tasks with severe label shift the proposed algorithm improves the accuracy and achieves the highest performance. DANN performs worse than a regular neural network under high label shift.

	U → M	M → U	0.3 → U	0.2 → U	0.1 → U
Source Accuracy	98.06	98.83	98.3	97.56	95.3
Domain Accuracy	46.4	50.63	50.42	50.48	50.44
1-NN Accuracy	-	-	77.89	73.22	69.75

Table 3: Source domain accuracy and domain classifier accuracy of DANN on MNIST-USPS tasks. The drop in source accuracy in cases of severe label shift is minimal compared to the drop in target accuracy in the previous table. The domain classifier accuracy is near random regardless of the amount of label shift. The performance of a nearest neighbor classifier trained on the mapped source data points and evaluated on the mapped target data points degrades to a large extent as label shift increases.

	en → bg	en → br	en → cn	en → da	en → de
No Adaptation (MSE)	55.22 (0.23)	53.51 (0.53)	4.48 (0.27)	64.75 (0.14)	47.95 (0.52)
No Adaptation (CE)	51.55 (0.12)	56.94 (0.04)	0.37 (0.00)	64.00 (0.18)	46.55 (0.22)
Conneau et al. (2018) (MSE)	46.88 (0.61)	46.20 (1.56)	53.54 (1.74)	51.98 (1.87)	50.43 (1.07)
Conneau et al. (2018) (CE)	45.12 (0.82)	36.96 (0.95)	49.87 (1.37)	50.99 (1.31)	43.62 (0.66)
Label Alignment Regularizer	59.85 (0.08)	53.42 (0.33)	65.10 (0.24)	65.58 (0.12)	60.46 (0.05)
	en → es	en → fr	en → he	en → hu	Average
No Adaptation (MSE)	39.17 (0.93)	49.89 (0.57)	58.19 (0.23)	59.66 (0.12)	48.09 (0.37)
No Adaptation (CE)	47.09 (0.20)	40.90 (0.36)	58.23 (0.10)	55.82 (0.06)	46.83 (0.10)
Conneau et al. (2018) (MSE)	48.37 (1.38)	46.45 (0.88)	48.93 (1.03)	47.15 (1.18)	48.88 (0.69)
Conneau et al. (2018) (CE)	41.30 (1.40)	44.18 (2.16)	46.95 (1.39)	44.06 (1.44)	44.78 (0.40)
Label Alignment Regularizer	43.47 (0.90)	58.11 (0.24)	61.24 (0.09)	59.68 (0.12)	58.55 (0.17)

Table 4: F_1 score in percents on different XED source-language pairs. MSE and CE denote Mean Squared Error and Cross Entropy loss. No Adaptation means that the model is trained directly on the source domain. The baseline by Conneau et al. (2018) is a domain-adversarial method. The proposed regularizer outperforms the baseline and direct training on the source domain on average and on most of the tasks.

representation-based domain adaptation method, with the hope that the hybrid method has the advantage of both—it can provide a significant advantage in a broad range of domain-shift settings, including the label shift. It would also be interesting to have a more rigorous theoretical characterization regarding when the label alignment property holds and to what extent the label vector can align with the top singular vectors.

References

David Acuna, Guojun Zhang, Marc T Law, and Sanja Fidler. f-domain adversarial learning: Theory and algorithms. In *International Conference on Machine Learning*, 2021.

Sanjeev Arora, Simon Du, Wei Hu, Zhiyuan Li, and Ruosong Wang. Fine-grained analysis of optimization and generalization for overparameterized two-layer neural networks. In *International Conference on Machine Learning*, 2019.

Aristide Baratin, Thomas George, César Laurent, R Devon Hjelm, Guillaume Lajoie, Pascal Vincent, and Simon Lacoste-Julien. Implicit regularization via neural feature alignment. In *International Conference on Artificial Intelligence and Statistics*, 2021.

Shai Ben-David, John Blitzer, Koby Crammer, Alex Kulesza, Fernando Pereira, and Jennifer Wortman Vaughan. A theory of learning from different domains. *Machine learning*, 2010.

- Sagie Benaim and Lior Wolf. One-sided unsupervised domain mapping. *Advances in neural information processing systems*, 2017.
- Thierry Bertin-Mahieux, Daniel P.W. Ellis, Brian Whitman, and Paul Lamere. The million song dataset. In *Proceedings of the 12th International Conference on Music Information Retrieval (ISMIR 2011)*, 2011.
- Christopher M Bishop and Nasser M Nasrabadi. *Pattern recognition and machine learning*, volume 4. Springer, 2006.
- Gilles Blanchard, Gyemin Lee, and Clayton Scott. Generalizing from several related classification tasks to a new unlabeled sample. *Advances in neural information processing systems*, 2011.
- Konstantinos Bousmalis, Nathan Silberman, David Dohan, Dumitru Erhan, and Dilip Krishnan. Unsupervised pixel-level domain adaptation with generative adversarial networks. In *IEEE conference on computer vision and pattern recognition*, 2017.
- Abdulkadir Canatar, Blake Bordelon, and Cengiz Pehlevan. Spectral bias and task-model alignment explain generalization in kernel regression and infinitely wide neural networks. *Nature communications*, 2021.
- Alexis Conneau, Guillaume Lample, Marc’Aurelio Ranzato, Ludovic Denoyer, and Hervé Jégou. Word translation without parallel data. In *International Conference on Learning Representations*, 2018.
- Nicolas Courty, Rémi Flamary, Amaury Habrard, and Alain Rakotomamonjy. Joint distribution optimal transportation for domain adaptation. *Advances in Neural Information Processing Systems*, 2017.
- Bharath Bhushan Damodaran, Benjamin Kellenberger, Rémi Flamary, Devis Tuia, and Nicolas Courty. Deepjdot: Deep joint distribution optimal transport for unsupervised domain adaptation. In *European Conference on Computer Vision*, 2018.
- Jacob Devlin, Ming-Wei Chang, Kenton Lee, and Kristina Toutanova. BERT: Pre-training of deep bidirectional transformers for language understanding. In *Proceedings of the 2019 Conference of the North American Chapter of the Association for Computational Linguistics: Human Language Technologies, Volume 1 (Long and Short Papers)*, 2019.
- Hadi Fanaee-T and Joao Gama. Event labeling combining ensemble detectors and background knowledge. *Progress in Artificial Intelligence*, 2014.
- Yaroslav Ganin, Evgeniya Ustinova, Hana Ajakan, Pascal Germain, Hugo Larochelle, François Laviolette, Mario Marchand, and Victor Lempitsky. Domain-adversarial training of neural networks. *The journal of machine learning research*, 2016.
- Muhammad Ghifary, W Bastiaan Kleijn, Mengjie Zhang, David Balduzzi, and Wen Li. Deep reconstruction-classification networks for unsupervised domain adaptation. In *European conference on computer vision*, 2016.
- Behnam Gholami, Pritish Sahu, Ognjen Rudovic, Konstantinos Bousmalis, and Vladimir Pavlovic. Unsupervised multi-target domain adaptation: An information theoretic approach. *IEEE Transactions on Image Processing*, 2020.
- Franz Graf, Hans-Peter Kriegel, Matthias Schubert, Sebastian Pölsterl, and Alexander Cavallaro. 2d image registration in ct images using radial image descriptors. In *International Conference on Medical Image Computing and Computer-Assisted Intervention*, 2011.
- Ishaan Gulrajani and David Lopez-Paz. In search of lost domain generalization. In *International Conference on Learning Representations*, 2021.
- Like Hui and Mikhail Belkin. Evaluation of neural architectures trained with square loss vs cross-entropy in classification tasks. In *International Conference on Learning Representations*, 2020.
- Ehsan Imani, Wei Hu, and Martha White. Representation alignment in neural networks. *Transactions on Machine Learning Research*, 2022.
- Arthur Jacot, Franck Gabriel, and Clément Hongler. Neural tangent kernel: Convergence and generalization in neural networks. *Advances in neural information processing systems*, 2018.
- Fredrik D Johansson, David Sontag, and Rajesh Ranganath. Support and invertibility in domain-invariant representations. In *The 22nd International Conference on Artificial Intelligence and Statistics*, 2019.
- Chen-Yu Lee, Tanmay Batra, Mohammad Haris Baig, and Daniel Ulbricht. Sliced wasserstein discrepancy for unsupervised domain adaptation. In *IEEE/CVF Conference on Computer Vision and Pattern Recognition*, 2019.
- Mingsheng Long, Yue Cao, Jianmin Wang, and Michael Jordan. Learning transferable features with deep adaptation networks. In *International conference on machine learning*, 2015.
- Mingsheng Long, Han Zhu, Jianmin Wang, and Michael I Jordan. Unsupervised domain adaptation with residual transfer networks. *Advances in neural information processing systems*, 2016.
- Mingsheng Long, Han Zhu, Jianmin Wang, and Michael I Jordan. Deep transfer learning with joint adaptation networks. In *International conference on machine learning*, 2017.
- Yishay Mansour, Mehryar Mohri, and Afshin Rostamizadeh. Domain adaptation: Learning bounds and algorithms. *Annual Conference on Learning Theory*, 2009.

- Zhong Meng, Jinyu Li, Yifan Gong, and Biing-Hwang Juang. Adversarial teacher-student learning for unsupervised domain adaptation. In *IEEE International Conference on Acoustics, Speech and Signal Processing*, 2018.
- Saeid Motiian, Quinn Jones, Seyed Iranmanesh, and Gianfranco Doretto. Few-shot adversarial domain adaptation. *Advances in neural information processing systems*, 2017.
- Emily Öhman, Marc Pàmies, Kaisla Kajava, and Jörg Tiedemann. XED: A multilingual dataset for sentiment analysis and emotion detection. In *Proceedings of the 28th International Conference on Computational Linguistics*, 2020.
- Guillermo Ortiz-Jiménez, Seyed-Mohsen Moosavi-Dezfooli, and Pascal Frossard. What can linearized neural networks actually say about generalization? *Advances in Neural Information Processing Systems*, 2021.
- Samet Oymak, Zalan Fabian, Mingchen Li, and Mahdi Soltanolkotabi. Generalization guarantees for neural networks via harnessing the low-rank structure of the jacobian. *arXiv*, 2019.
- Pau Panareda Busto and Juergen Gall. Open set domain adaptation. In *IEEE international conference on computer vision*, 2017.
- Karl Pearson. Liii. on lines and planes of closest fit to systems of points in space. *The London, Edinburgh, and Dublin philosophical magazine and journal of science*, 2(11):559–572, 1901.
- Zhongyi Pei, Zhangjie Cao, Mingsheng Long, and Jianmin Wang. Multi-adversarial domain adaptation. In *Thirty-second AAAI conference on artificial intelligence*, 2018.
- Xue Bin Peng, Marcin Andrychowicz, Wojciech Zaremba, and Pieter Abbeel. Sim-to-real transfer of robotic control with dynamics randomization. In *IEEE international conference on robotics and automation*, 2018.
- Telmo Pires, Eva Schlinger, and Dan Garrette. How multilingual is multilingual BERT? In *Proceedings of the 57th Annual Meeting of the Association for Computational Linguistics*, 2019.
- Nasim Rahaman, Aristide Baratin, Devansh Arpit, Felix Draxler, Min Lin, Fred Hamprecht, Yoshua Bengio, and Aaron Courville. On the spectral bias of neural networks. In *International Conference on Machine Learning*, 2019.
- Sylvestre-Alvise Rebuffi, Hakan Bilen, and Andrea Vedaldi. Learning multiple visual domains with residual adapters. *Advances in neural information processing systems*, 2017.
- Kuniaki Saito, Yoshitaka Ushiku, and Tatsuya Harada. Asymmetric tri-training for unsupervised domain adaptation. In *International Conference on Machine Learning*, 2017.
- Hidetoshi Shimodaira. Improving predictive inference under covariate shift by weighting the log-likelihood function. *Journal of statistical planning and inference*, 2000.
- Baochen Sun and Kate Saenko. Deep coral: Correlation alignment for deep domain adaptation. In *European conference on computer vision*, 2016.
- Eric Tzeng, Judy Hoffman, Ning Zhang, Kate Saenko, and Trevor Darrell. Deep domain confusion: Maximizing for domain invariance. *arXiv*, 2014.
- Chiyuan Zhang, Samy Bengio, Moritz Hardt, Benjamin Recht, and Oriol Vinyals. Understanding deep learning requires rethinking generalization. In *International Conference on Learning Representations*, 2017a.
- Yuan Zhang, Regina Barzilay, and Tommi Jaakkola. Aspect-augmented adversarial networks for domain adaptation. *Transactions of the Association for Computational Linguistics*, 2017b.
- Yuchen Zhang, Tianle Liu, Mingsheng Long, and Michael Jordan. Bridging theory and algorithm for domain adaptation. In *International Conference on Machine Learning*, 2019.
- Han Zhao, Remi Tachet Des Combes, Kun Zhang, and Geoffrey Gordon. On learning invariant representations for domain adaptation. In *International Conference on Machine Learning*, 2019.
- Fuzhen Zhuang, Xiaohu Cheng, Ping Luo, Sinno Jialin Pan, and Qing He. Supervised representation learning: Transfer learning with deep autoencoders. In *Twenty-Fourth International Joint Conference on Artificial Intelligence*, 2015.
- Fuzhen Zhuang, Xiaohu Cheng, Ping Luo, Sinno Jialin Pan, and Qing He. Supervised representation learning with double encoding-layer autoencoder for transfer learning. *ACM Transactions on Intelligent Systems and Technology*, 2017.

A Proofs

A.1 Label Alignment Property

We show that label alignment emerges if multiple features are highly correlated with the labels.

Lemma 3 *If there are $k' < d$ orthonormal vectors $\{\nu_1, \dots, \nu_{k'}\}$ such that $\|\Phi\nu_i\| < \epsilon$ for all $i \in [k']$ then $\Phi_{n \times d}$ has at most $d - k'$ singular values greater than or equal to $\sqrt{k'}\epsilon$.*

Proof Suppose $\sigma_1, \dots, \sigma_d$ are the singular values of Φ sorted in descending order. The matrix $N_{d \times k'}$ with orthonormal columns that minimizes $\|\Phi N\|_2$ is the matrix of the last k' right singular vectors, and $\|\Phi N\|_2 = \sqrt{\sum_{i=d-k'+1}^d \sigma_i^2} \geq \sigma_{d-k'+1}$ (This easily follows from Section 12.1.2 by Bishop & Nasrabadi (2006)). If $\sigma_{d-k'+1} \geq \sqrt{k'}\epsilon$ then for any N with orthonormal columns we have $\|\Phi N\|_2 \geq \sqrt{k'}\epsilon \implies \|\Phi N\|_\infty \geq \epsilon$ which contradicts the assumption. ■

Proposition 4 *Suppose $\|y\| = 1$ and that columns of Φ are normalized. If $\Phi_{n \times d}$ has $\hat{k} \leq d$ columns $\{\Phi_{:,1}, \dots, \Phi_{:,\hat{k}}\}$ where $|\Phi_{:,i}^\top y| > 1 - \delta$ for all $i \in [\hat{k}]$ and*

- $0 < \delta < 0.2$
- $\hat{k} > 16\delta^2 / (-15\delta^2 - 2\delta + 1)$
- $d > 16\delta^2(\hat{k} - 1)$

then the norm of the projection of y on the span of the first $k = d - \hat{k} + 1$ left singular vectors of Φ is greater than

$$\sqrt{\frac{\hat{k}(1 - \delta)^2 - 16\delta^2(\hat{k} - 1)}{d - 16\delta^2(\hat{k} - 1)}}$$

Proof First suppose the dot products in the statement are positive.

Note that for all $i \in \hat{k}$ we have $\|\Phi_{:,i} - y\|_2^2 = (\Phi_{:,i} - y)^\top (\Phi_{:,i} - y) = \Phi_{:,i}^\top \Phi_{:,i} + y^\top y - 2\Phi_{:,i}^\top y = 2 - 2\Phi_{:,i}^\top y < 2\delta$. Due to triangle inequality, $\|\Phi_{:,i} - \Phi_{:,j}\|_2^2 \leq \|\Phi_{:,i} - y\|_2^2 + \|\Phi_{:,j} - y\|_2^2 < 4\delta$.

The span of $\Phi_{:, \hat{k}}, \Phi_{:, \hat{k}+1}, \dots, \Phi_{:, d}$ has at most $d - \hat{k} + 1$ dimensions. Choose $\hat{k} - 1$ orthonormal vectors $\nu_1, \dots, \nu_{\hat{k}-1} \in \mathbb{R}^d$ that are perpendicular to this subspace. Then for any $i, j \in [\hat{k} - 1]$ we have $\Phi_{:,i}^\top \nu_j = (\Phi_{:,i} - \Phi_{:, \hat{k}} + \Phi_{:, \hat{k}})^\top \nu_j = (\Phi_{:,i} - \Phi_{:, \hat{k}})^\top \nu_j + 0 \leq \|\Phi_{:,i} - \Phi_{:, \hat{k}}\| < 4\delta$. Therefore $\|\Phi\nu_j\| < 4\delta\sqrt{\hat{k} - 1}$. Putting this orthonormal basis in the lemma above gives that Φ has at most $d - \hat{k} + 1$ singular values greater than or equal to $4\delta(\hat{k} - 1)$.

Now see that $\|\Phi^\top y\|^2 = \left\| \sum_{i=1}^d \Phi_{:,i}^\top y \right\|^2$ and is also equal to $\sum_{i=1}^d (\sigma_i y_i^U)^2$. Therefore $\sum_{i=1}^d (\sigma_i y_i^U)^2 \geq \left\| \sum_{i=1}^{\hat{k}} \Phi_{:,i}^\top y \right\|^2 > \hat{k}(1 - \delta)^2$. Since the columns are normalized, $\sum_{i=1}^d \sigma_i^2 = \|\Phi\|_F^2 = d$. In addition we have shown that the last $\hat{k} - 1$ singular values are smaller than $4\delta\sqrt{\hat{k} - 1}$. Define \hat{y} as the projection of y on the first $d - \hat{k} + 1$ singular vectors of Φ . Then we have $\hat{k}(1 - \delta)^2 < \sum_{i=1}^d (\sigma_i y_i^U)^2 = \sum_{i=1}^{d-\hat{k}+1} (\sigma_i y_i^U)^2 + \sum_{i=d-\hat{k}+2}^d (\sigma_i y_i^U)^2 < d\|\hat{y}\|^2 + 16\delta^2(\hat{k} - 1)(1 - \|\hat{y}\|^2)$. Rearranging the terms (with the extra conditions in the proposition statement) gives

$$\|\hat{y}\| > \sqrt{\frac{\hat{k}(1 - \delta)^2 - 16\delta^2(\hat{k} - 1)}{d - 16\delta^2(\hat{k} - 1)}}$$

The inequality is tight in the extreme case where $\hat{k} = d$ and $\delta \rightarrow 0$ which results in the label vector being fully in the direction of the first left singular vector and all the other singular values tending to zero.

Now suppose some of the dot products in the statement are negative. We can multiply those columns with -1 and prove the result above for this modified matrix. The result holds for the original matrix since this operation only changes the right

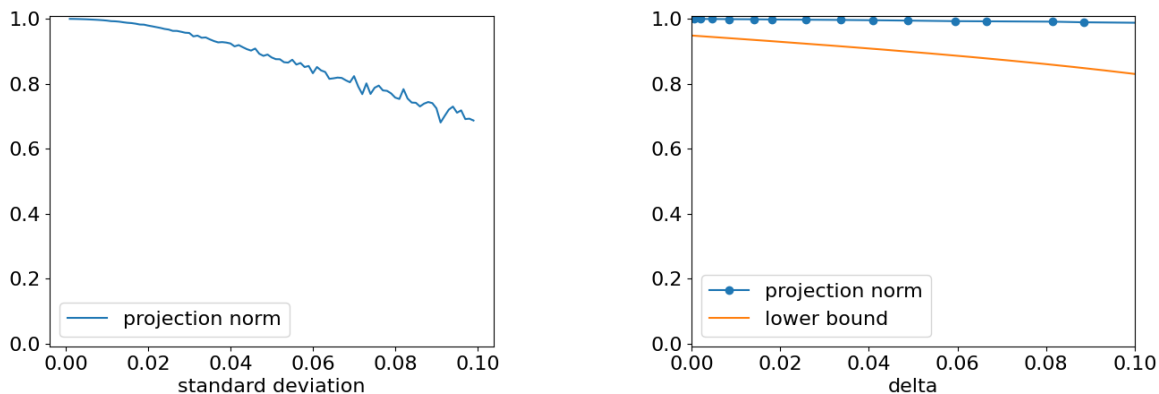


Figure 2: Projection of the label vector on the top two singular vectors in the Gaussian example. For small values of standard deviation (where the labels are highly correlated with the features) and small values of δ , the label vector is mostly in the direction of the top two singular vectors. The lower bound is applicable in this regime and is close to one.

singular vectors of Φ and does not affect the left singular vectors or the singular values. ■

Let us demonstrate emergence of alignment and the behavior of the bound when multiple features are highly correlated with the output. In this toy experiment the label vector is sampled from a 1000 dimensional Gaussian distribution $\mathcal{N}(\mathbf{0}, \mathbb{I})$ with mean zero and standard deviation 1 and then normalized to norm one. The matrix Φ has 10 columns. The first 9 columns are sampled from $\mathcal{N}(y, s^2\mathbb{I})$ with mean y and a small standard deviation s and the other column is sampled from $\mathcal{N}(\mathbf{0}, \mathbb{I})$. All columns are then normalized to norm one. Figure 2 shows the norm of the projection of the label vector on the first two singular vectors at different levels of s and its relationship with δ .

B Experiment Details

This Section outlines dataset details, hyperparameter settings, and other design choices in the experiments.

Label Alignment in Real-World Tasks. We used the following tasks in this experiment:

1. **UCI CT Scan:** A random subset of the CT Position dataset on UCI (Graf et al., 2011). The task is predicting a location of a CT Slice from histogram features.
2. **Song Year:** A random subset of the training portion of the Million Song dataset (Bertin-Mahieux et al., 2011). The task is predicting the release year of a song from audio features.
3. **Bike Sharing:** A random subset of the Bike Sharing dataset on UCI (Fanaee-T & Gama, 2014). The task is predicting the number of rented bikes in an hour based on information about weather, date, and time.
4. **MNIST:** The task is classifying digits 0 and 1 in MNIST.
5. **USPS:** The task is classifying digits 0 and 1 in USPS.
6. **CIFAR-10:** The task is classifying airplane and automobile in CIFAR-10 dataset using features from a ResNet-18 pretrained on ImageNet.
7. **CIFAR-100:** The task is classifying beaver and dolphin in CIFAR-100 dataset using features from a ResNet-18 pretrained on ImageNet.
8. **STL-10:** The task is classifying airplane and bird in STL-10 dataset using features from a ResNet-18 pretrained on ImageNet.
9. **XED (English):** The English corpus from XED datasets whose details are discussed in the main paper. The features are sentence embeddings extracted from BERT.

10. **AG News:** A random subset of the first two classes (World and Sports) in AG News document classification dataset. The features are obtained by feeding the document text to BERT.

All datasets have an extra constant 1 feature to account for the bias unit. Rank is computed as the number of singular values larger than $\sigma_1 * \max(n, d) * 1.19209e - 07$. This is the default numerical rank computation method in the Numpy package.

MNIST-USPS. DANN uses a one-layer ReLU neural network. This is the Shallow DANN architecture suggested by the original authors (Ganin et al., 2016). We swept over values of 128, 256, 512, and 1024 for the depth of the hidden layer.

The neural network is trained for 10 epochs using SGD with batch size 32, learning rate 0.01, and momentum 0.9. This model already achieves near perfect accuracy on the source domain.

Candidate hyperparameter values for Label Alignment Regularizer were $1e - 1, 1e + 1, 1e + 3$ for λ and $8, 16, 32, \dots$ up to the rank of Φ or $\tilde{\Phi}$ for k and \tilde{k} .

Although the number of hyperparameter configurations is greater for our method, this experiment is in favor of DANN if we take runtime into account.

The linear model is trained using full-batch gradient descent for 5000 epochs with learning rate $1/(2\sigma_1)$.

Sentiment Classification. For the domain-adversarial baseline (Conneau et al., 2018) we sweep over values of $1e - 3, 1e - 2, 1e - 1$ for β . The parameter controls the degree of orthogonality of the transformation that maps the source and target embeddings into a common space.

Candidate hyperparameter values for Label Alignment Regularizer were $1e - 1, 1e + 1, 1e + 3$ for λ and $8, 16, 32, \dots$ up to the rank of Φ or $\tilde{\Phi}$ for k and \tilde{k} .

Similar to the previous experiment, the hyperparameter grid search in this experiment is in favor of the baseline if we take runtime into account.

All models in this section are linear regression and logistic regression (on the nonlinear extracted representations). The models are trained with learning rate $1/(2\sigma_1)$ (MSE loss) and $1e - 2$ (CE loss) and momentum 0.9.

C Additional Experiments

We create a regression task similar to the synthetic experiment in the main paper. The aim is to understand if results similar to the synthetic experiment hold in a setting where the labels are not restricted to ± 1 and where mean squared error is used for evaluation. All the details are the same as in the classification experiment in the main paper except that the label vector is simply set to the first left singular vector. Figure 3 shows the results and corroborates the findings in the main paper. Note that DANN is not directly applicable here.

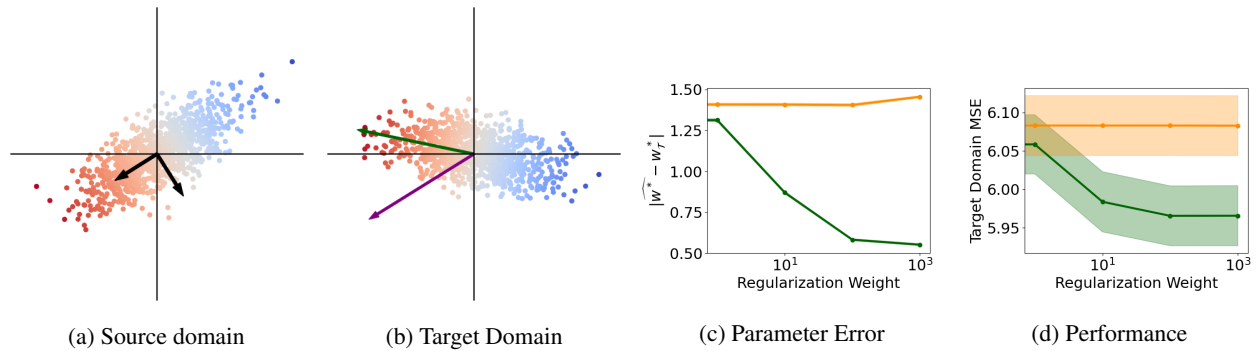


Figure 3: (a) Source domain. The black arrows show principal components. (b) Target domain. The arrows show weights found without using any regularization (purple) and with our regularizer with $\lambda = 10^3$ (green). (c) Distance between the estimated and the optimal weights. The proposed regularizer reduces this distance. (d) Performance on the target domain. The x axis is the regularization coefficient for ℓ_2 regularization and λ for the proposed regularizer. The proposed regularizer achieves lower error on this domain. Shaded areas are standard errors over 10 runs.